energies

MDPI

Article

Assessing the Exergetic and Inherent Safety Performance of a Shrimp-Based Biorefinery via Computer-Aided Tools

Kariana Andrea Moreno-Sader [1], Jairo David Martínez-Consuegra [2] and Ángel Darío González-Delgado [1,*]

[1] Nanomaterials and Computer-Aided Process Engineering Research Group (NIPAC), Chemical Engineering Department, University of Cartagena, Consulado Avenue St. 30, Cartagena 48-152, Bolívar, Colombia; kmorenos@unicartagena.edu.co

[2] Corporación Universitaria Minuto de Dios, Cra. 53, Barranquilla 74-110, Atlántico, Colombia; jairo.martinezc@uniminuto.edu

* Correspondence: agonzalezd1@unicartagena.edu.co

Received: 3 July 2020; Accepted: 12 November 2020; Published: 18 December 2020

Abstract: Although shrimp processing wastes have been studied as source of high-value products at lab-scale, no contributions are found in the literature regarding the energetic and safety performance of shrimp-based biorefineries at pilot or large-scale. This works is focused on the inherent safety assessment and exergy analysis of a pilot-scale biorefinery designed to produce shrimp meat and four by-products: chitin, chitosan, nitrogenous extract, and astaxanthin. Total irreversibilities, exergy losses, exergy of wastes and utilities were calculated for stages and the overall process using mass and energy balances of the biorefinery. The hazards associated with chemicals and process conditions were analyzed through substance properties and process data. A Numerical Descriptive Inherent Safety Technique (*NuDIST*) score of 557.23 suggested a moderate level of risk for the biorefinery compared to other processes, reaching chemical and process safety scores of 185.88 and 371.35, respectively. Sections (b) and (c) were identified as major hotspots from a safety point of view. The overall exergy efficiency was quantified at 25.61%, which is higher than the chitosan-from-exoskeleton linear production chain (4.58%). The highest exergy losses were found on stages as deacetylation, fresh shrimp washing and deproteinization stages. The beheading stage most contributed to irreversibilities, with 98.315%, followed by sorting, with 1.653%. These results could identify opportunities for improvement from an exergy and safety point of view by mapping less efficient and hazardous stages.

Keywords: biorefinery; shrimp; safety; exergy

1. Introduction

The production of shrimp has shown an increasing trend in recent years of up to 6% annual, which accounted for 4 million tons of farmed shrimp by 2018 [1]. As the market preference is peeled undeveined shrimp, around 45–48% of the fresh shrimp weight is discharged during processing, and consequently, a large amount of waste is generated and disposed of into landfills or back into the ocean [2]. Such shrimp wastes (SWs) are rich source of natural compounds like chitin, astaxanthin, proteins and lipids that have numerous applications in agriculture, food, medical, pharmaceutical, textile and water treatment [3]. To extract these biomaterials, different conventional and non-conventional techniques are used at laboratory scale (e.g., maceration, microwave-assisted extraction, solvent extraction, Soxhlet extraction, supercritical fluid extraction) [4]. Chitin is commonly isolated via chemical methods using solvent mixtures; however, promising technologies that combine microwave energy and ionic liquids have reported a higher molecular weight and purity [5]. The isolation of

carotenoids has been addressed via supercritical fluid extraction (SFE), subcritical water extraction, and extraction with solvents such as acetone and ionic liquids [6,7]. The SFE technology offers advantages over conventional methods to improve the isolation selectivity and prevent solvent traces in the final product [8]. Despite the drawbacks of chemical-based extraction, organic solvents are still used in multistep chemical processes for high-value product extraction and recovery from marine biowaste.

The biorefinery concept is recognized as a strategic mechanism of circular economy to transform biomass into marketable food, material and energy [9]. Driven by the sustainable performance of biorefinery systems, several technologies are proposed for feedstocks including lignocellulosic biomass, algal biomass, food wastes, shrimp and crustacean shells, microbial treated wastes [10]. Lignocellulosic biomasses are of particular interest due to their high quantity availability and use as a source of bioenergy [11]; however, the increasing demand for natural sources for bioactive compounds has motivated research in crustacean-based biorefineries. A biorefinery approach within the shrimp industry is expected to impact the market for biocompounds in coming years [5], where meat is produced while providing chitin, chitosan and astaxanthin from biowastes. Despite recent progress in shrimp-based biorefineries, more research is needed on the implementation of a biorefinery that can fulfill the gap between current processing and the existing knowhow on compound extraction from biowastes.

The sustainability of biorefinery systems is assessed via methodologies such as techno-economic assessment, exergy analysis, life-cycle assessment, a waste reduction algorithm and inherent safety [12,13]. The exergy approach has been widely used to analyze and improve processes since it enables the identification of energy degradation by measuring losses and irreversibilities [14]. Exergy efficiency is defined as the ratio of exergy output rate to exergy input rate [15]. This could be a more important indicator than energy efficiency, revealing the quality of energy used in the system [16]. The inherent safety approach is also a powerful assessing tool that enables the identification of potential risks at early design phase of biorefineries in order to locate improvement opportunities that may reduce either the probability or severity of risk occurrence [17].

Recent works have addressed the exergetic performance of different types of biorefineries, for example, Ofori-Boateng (2014) [18] evaluated the sustainability of a palm-oil-based biorefinery producing cellulosic ethanol and phytochemicals using exergetic life cycle assessment. They reported exergy efficiency and thermodynamic sustainability index (TSI) at 59.05% and 2.44, respectively; this approach identified major areas where improvements are needed for sustainable production of biofuels and biochemicals. A lignocellulosic biorefinery coupled to a sugarcane mill was also explored via exergy analysis, showing efficiency of 44.73% and exergy losses from steam generator [19]. Meramo et al. (2020) [1] studied the linear-chain production of chitosan from shrimp exoskeleton and achieved an overall exergy efficiency of 4.58%. They found the highest irreversibilities in the depigmentation stages, concluding that design improvements may increase up to 58.93% the overall efficiency.

Compared with the traditional chemical and petrochemical plants, the biorefinery designs have fewer advances in terms of safety aspects, and there are still limited data on risk assessment and management [20]. Roberto Lauri and Biancamaria Pietrangeli (2019) [21] identified safety issues in a biorefinery approach for bioethanol production, highlighting hazards associated with the handling of biofuel and emission sources in case of component failure. Meramo et al. (2020) [22] carried out the synthesis and sustainability evaluation of a lignocellulosic multifeedstock biorefinery considering environmental, economic and safety indicators, reporting an sustainability return on an investment of 27.29%. Pinedo et al. (2016) [23] applied Preliminary Hazard Analysis (PHA) and Event Tree Analysis (ETA) to estimate the consequences and frequencies of risks in microalgae biorefinery alternatives, finding major consequences of accidents in the release of n-hexane.

Driven by the marginal tracking of exergetic and safety aspects in the design of shells biorefineries, this work aims to study the performance of a shrimp biorefinery for meat, chitin, chitosan, astaxanthin and nitrogenous extract production using inherent safety methodology and exergy

analysis, which enable the identification of the improvements required for a more sustainable design of this biorefinery at pilot-scale.

2. Materials and Methods

2.1. Process Description

This biorefinery was designed to process 4534 tons/y of fresh shrimp corresponding to the farmed shrimp rate in North Colombia in 2018 [24]. Experimental data previously obtained at lab-scale [25] for chitosan and astaxanthin production were used to perform the mass and energy balances. The biorefinery is divided into four main sections: (a) *Shrimp processing* where shrimp meat is obtained, (b) *Shrimp shells processing* and chitin recovery, (c) *Chitosan production* and (d) *Astaxanthin recovery*, which are shown in Figures 1–4. The main subsections are numbered for further analysis using computer-aided tools (see Table 1).

Table 1. Stages' nomenclature in shrimp-based biorefinery.

Section	Stage No.	Stage Name
(a) Shrimp processing	1	Fresh shrimp washing
	2	Sorting
	3	Beheading
	4	Peeling
(b) Shrimp shells' processing and chitin recovery	5	Shrimp shell pretreatment
	6	Depigmentation 1
	7	Demineralization
	8	Deproteinization
	9	Chitin purification
(c) Chitosan production	10	Deacetylation
	11	Chitosan purification
(d) Astaxanthin recovery	12	Depigmentation 2
	13	Astaxanthin purification

Shrimp processing: This section covers those stages where fresh shrimp is processed to obtain shrimp meat. As shown in Figure 1, farmed shrimps are washed using 50% ice water along with 10 ppm chlorine solution and 8% vol. metabisulfite solution [26]. Chlorine serves as a bactericidal agent, while metabisulfite serves as a preservative by preventing shrimp from staining [27]. The shrimps undergo a sorting stage where a visual inspection enables the separation of damaged, with defects such as discoloration or deterioration, from qualified shrimp. The latter is sent to the beheading and peeling stages to obtain peeled undeveined product following market specifications. The biowaste stream from peeling feeds into the pretreatment unit in Section (b). Table 2 summarizes the process data for the shrimp processing section.

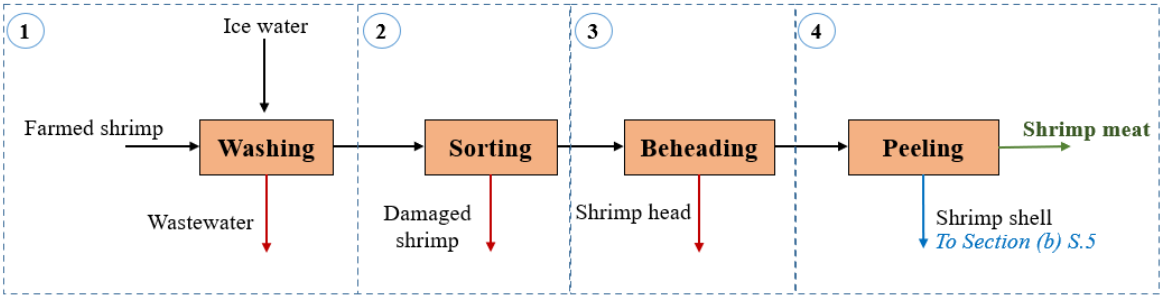

Figure 1. Block diagram of the shrimp processing section in the shrimp-based biorefinery.

Table 2. Mass composition of main streams for section (a).

Operating Conditions	Farmed Shrimp	Wastewater	Damaged Shrimp	Shrimp Shells	Shrimp Meat
Temperature (°C)	9	9	9	9	−18
Pressure (atm)	1	1	1	1	1
Mass flow (kg/h)	469.22	124.73	2.35	49.02	277.79
			Composition (wt.)		
L-alanine-N-L-alanyl	0.035	0.000	0.036	0.036	0.035
L-glutamic acid	0.061	0.000	0.062	0.062	0.061
L-phenylalanine	0.023	0.000	0.023	0.023	0.023
Methionine	0.021	0.000	0.021	0.021	0.020
Lysine	0.067	0.000	0.068	0.068	0.066
$CaCO_3$	0.018	0.000	0.029	0.029	0.010
$Ca_3(PO_4)_2$	0.044	0.000	0.072	0.072	0.026
Na_2CO_3	0.009	0.000	0.015	0.015	0.005
$MgCO_3$	0.005	0.000	0.008	0.008	0.003
D-N-acetylglucosamine	0.068	0.000	0.167	0.167	0.000
Methyl-palmitate	0.123	0.000	0.293	0.293	0.006
Astaxanthin	0.001	0.000	0.002	0.002	0.000
Water	0.524	0.975	0.204	0.204	0.745
Sodium metabisulfite	0.000	0.025	0.000	0.000	0.000

Shrimp shells processing and chitin recovery: The stages ascribed to this section attempt to process shells for further isolation of chitin and nitrogenous extract (Figure 2). Shrimp shells are washed to remove organic matter, followed by drying until constant weight, and crushing to particle size at 0.5 mm [25]. In this biorefinery approach, we introduced a centrifugation stage before drying at 65 °C to remove excess water. This enables lower moisture content in the pretreated shells while maintaining adequate thermal efficiency [28]. The mainstream is sent to the depigmentation stage where astaxanthin is separated using 85% vol. ethanol [25]. The calcium carbonate and other minerals in the shells are removed by a demineralization stage with dilute hydrochloric acid at 1.5 M. Reactions (1)–(4) take place during demineralization of shells, followed by washing and neutralization [29]. The demineralized shells are sent to a deproteinization stage using 1.0 M sodium hydroxide solution around 80–90 °C to separate chitin from proteins, followed by water washing until neutral pH [25]. The resulting stream is divided into equal parts: 50% chitin is sent to *chitosan production* section and the other half is dried above 60 °C for selling purposes. The residue leaving the deproteination stage is rich in nitrogen, thus, it can be employed as nitrogenous extract for commercial applications in microalgae cultures. Table 3 lists the mass composition of main streams entering and leaving this section.

$$CaCO_3 + 2\,HCl \rightarrow CaCl_2 + H_2O + CO_2 \quad \text{(Reaction 1)}$$

$$Na_2CO_3 + 2\,HCl \rightarrow 2\,NaCl + H_2O + CO_2 \quad \text{(Reaction 2)}$$

$$MgCO_3 + 2\,HCl \rightarrow MgCl_2 + H_2O + CO_2 \quad \text{(Reaction 3)}$$

$$Ca_3(PO_4)_2 + 6\,HCl \rightarrow 3\,CaCl_2 + 2\,H_3PO_4 \quad \text{(Reaction 4)}$$

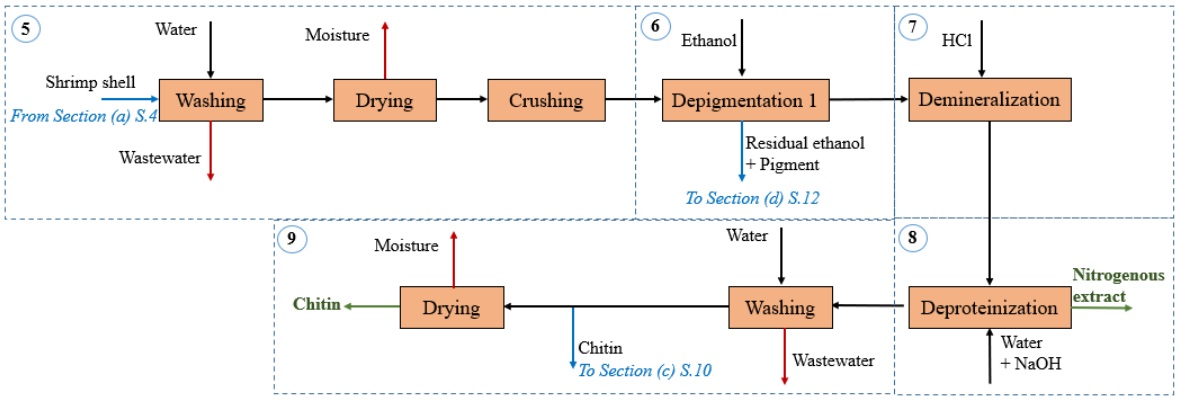

Figure 2. Block diagram of the shrimp shells processing and chitin recovery section in the shrimp-based biorefinery.

Table 3. Mass composition of main streams for section (b).

Operating Conditions	Ethanol	Residual Ethanol + Pigment	Wastewater	Nitrogenous Extract	Chitin
Temperature (°C)	25	25	25	90	100
Pressure (atm)	1	1	1	1	1
Mass flow (kg/h)	168.35	168.95	2389.081	460.44	3.336
			Composition (wt.)		
L-alanine-N-L-alanyl	0.000	0.000	0.000	0.004	0.000
L-glutamic acid	0.000	0.000	0.000	0.007	0.000
L-phenylalanine	0.000	0.000	0.000	0.002	0.000
Methionine	0.000	0.000	0.000	0.002	0.000
Lysine	0.000	0.000	0.000	0.007	0.000
D-N-acetylglucosamine	0.000	0.000	0.000	0.000	1.000
Methyl-palmitate	0.000	0.000	0.006	0.000	0.000
Astaxanthin	0.000	0.001	0.000	0.000	0.000
Water	0.150	0.152	0.980	0.963	0.000
Ethanol	0.850	0.847	0.000	0.000	0.000
Carbon dioxide	0.000	0.000	0.000	0.000	0.000
Magnesium chloride	0.000	0.000	0.000	0.000	0.000
Calcium chloride	0.000	0.000	0.002	0.000	0.000
Orto phosphoric acid	0.000	0.000	0.001	0.000	0.000
Sodium chloride	0.000	0.000	0.011	0.000	0.000
Sodium hydroxide	0.000	0.000	0.000	0.015	0.000

Chitosan production: Figure 3 depicts the block diagram of this section covering those stages where chitin is transformed into chitosan. The chitin from *Shrimp shells processing* section is sent to a deacetylation stage where the reaction (5) takes place [30], and high degrees of deacetylation are achieved at high temperatures (above 100 °C) in an alkaline medium at 50% *w*/*v* sodium hydroxide [2,25]. The chitosan stream is then purified by washing and drying stages. The deacetylation degree of chitosan from shell is around 81.81 based on the experimental results, supporting this pilot-scale approach [25]. The mass balance for Section (c) is summarized in Table 4.

$$C_8H_{15}NO_6 + NaOH \rightarrow C_6H_{13}NO_5 + C_2H_3NaO_2 \quad \text{(Reaction 5)}$$

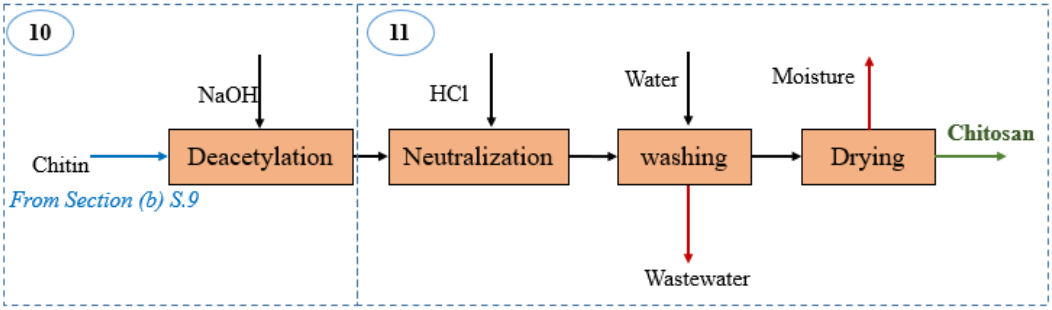

Figure 3. Block diagram of the chitosan production section in the shrimp-based biorefinery.

Table 4. Mass composition of main streams for section (c).

Operating Conditions	NaOH	HCl	Water	Wastewater	Chitosan
Temperature (°C)	25	25	25	25	25
Pressure (atm)	1	1	1	1	1
Mass flow (kg/h)	212.8	341.7	305.15	1003.44	2.70
			Composition (wt.)		
Water	0.980	0.969	1.000	0.987	0.000
Hydrochloric acid	0.000	0.031	0.000	0.007	0.000
Sodium chloride	0.000	0.000	0.000	0.005	0.000
Chitosan	0.000	0.000	0.000	0.000	1.000
Sodium acetate	0.000	0.000	0.000	0.001	0.000
Sodium hydroxide	0.020	0.000	0.000	0.000	0.000

Astaxanthin recovery: This section encompasses the isolation of astaxanthin from the pigment-rich stream leaving the depigmentation stage in Section (b). As shown in Figure 4, such a mixture is subjected to a second stage of depigmentation using 10% *v*/*v* acetone [25]. The resulting stream enters a separation train consisting of centrifugation, evaporation and drying stage at temperatures around 45 °C to obtain 0.11 kg/h of pure astaxanthin for further selling. Table 5 reports the mass balance around Section (d).

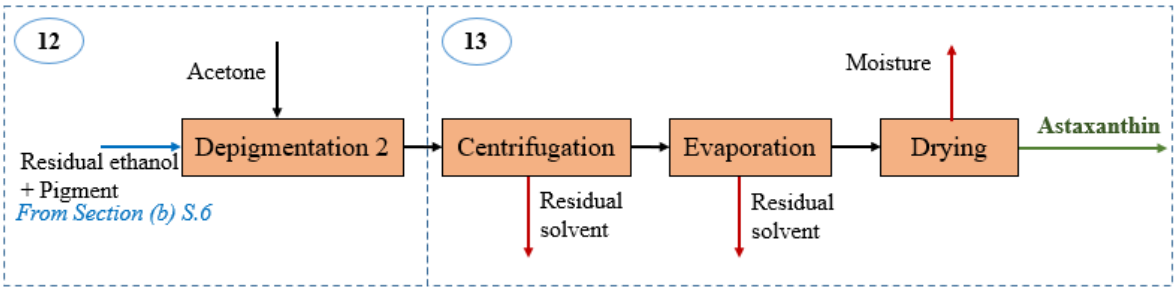

Figure 4. Block diagram of *astaxanthin recovery* section in the shrimp-based biorefinery.

Table 5. Mass composition of main streams for section (d).

Operating Conditions	Acetone	Residual Solvent from Centrifugation	Residual Solvent from Evaporation	Astaxanthin
Temperature (°C)	25	25	25	25
Pressure (atm)	1	1	1	1
Mass flow (kg/h)	19.97	190.36	0.147	0.112463
		Composition (wt.)		
Astaxanthin	0.000	0.000	0.000	1.000
Water	0.920	0.231	0.000	0.000
Ethanol	0.000	0.761	0.989	0.000
Acetone	0.080	0.008	0.011	0.000

2.2. Exergy Analysis

Exergy analysis was applied assuming that the whole process is in steady state, kinetic exergy and potential exergy is neglected, and temperature of reference is 298 K.

Governing equations: Exergetic analysis is governed by the equations described below [31,32]. There is an exergy loss in the exergy balance associated with system irreversibilities, corresponding to an estimate of the amount of destroyed exergy that flows throughout a bounded system [1]. Overall exergy balance is given by Equation (1), where $\left(\dot{E}x_{mass,in}\right)$ and $\left(\dot{E}x_{mass,out}\right)$ refer to exergy of inlet and outlet streams across the boundary, respectively.

$$\dot{E}x_{loss} = \dot{E}x_{mass,in} - \dot{E}x_{mass,out} + \dot{E}x_{heat} - \dot{E}x_{work} \quad (1)$$

$\dot{E}x_{heat}$ is the exergy by heat flow which is estimated by Carnot expression, as shown in Equation (2), considering heat flow $(\dot{Q})$, temperature (T), and temperature of reference (T_0). According to Equation (3), exergy by work $(\dot{E}x_{work})$ is equal to the workflow of the system $(\dot{W})$.

$$\dot{E}x_{heat} = \left(1 - \frac{T_0}{T}\right)\dot{Q} \quad (2)$$

$$\dot{E}x_{work} = \dot{W} \quad (3)$$

The mass exergy component $(\dot{E}x_{mass})$ is composed of physical $(\dot{E}x_{phy})$, chemical $(\dot{E}x_{chem})$, potential $(\dot{E}x_{pot})$ and kinetic $(\dot{E}x_{kin})$ exergies, as described by Equation (4). Based on the assumptions, kinetic and potential exergies are negligible compared to chemical and physical exergies.

$$\dot{E}x_{mass} = \dot{E}x_{phy} + \dot{E}x_{chem} - \dot{E}x_{pot} - \dot{E}x_{kin} \quad (4)$$

Chemical exergy of a process stream is shown by Equation (5), which depends on the chemical exergy $(Ex^0_{ch,i})$ of each component i in the mixture and its molar fraction (y_i). This also includes the gas constant R and temperature of reference, T_0. The chemical exergy of a component is generally available in the literature; however, for some substances, it is calculated by Equation (6)

$$\dot{E}x_{ch,mx} = \sum_i y_i Ex^0_{ch,i} + RT_0 \sum_i y_i \ln(y_i) \quad (5)$$

$$Ex^0_{ch,i} = \Delta G^0_{f,i} + \sum_j n_j Ex^0_{ch,j} \quad (6)$$

where (n_j) is the number of atoms of elements j in component i, $(Ex^0_{ch,j})$ is the chemical exergy of elements j, $\left(\Delta G^0_{f,i}\right)$ is the Gibbs free energy of formation of component i.

Physical exergy flow is given by Equation (7) that relates to system enthalpy (H) and entropy (S) at current temperature and pressure, and reference conditions $\left(\dot{H}_0, \dot{S}_0\right)$. For gases and solid–liquid mixture, this equation is transformed into Equations (8) and (9), respectively,

$$\dot{E}x_{phy} = \left(\dot{H} - \dot{H}_0\right) + T_0\left(\dot{S} - \dot{S}_0\right) \tag{7}$$

$$\dot{E}x_{phy} = C_P(T - T_0) - T_0\left(C_P \ln \frac{T}{T_0} - R \ln \frac{P}{P_0}\right) \tag{8}$$

$$\dot{E}x_{phy,liq-sol} = C_P\left[(T - T_0) - T_0 \ln \frac{T}{T_0}\right] - v_m(P - P_0) \tag{9}$$

where (C_P) is the heat capacity, (v_m) the molar volume, (P) the operating pressure, and (P_0) the reference pressure. In this work, the physical exergy of each process stream was obtained from Aspen Plus® software for a given pressure, temperature, and composition. The Non-Random Two Liquid (NRTL) model was selected to estimate thermodynamic properties.

A balance around the system provides the total exergy entering by mass $(\dot{E}x_{mass,in})$ and utilities $\left(\dot{E}x_{utilities,in}\right)$ [32]

$$\dot{E}x_{in} = \dot{E}x_{mass,in} + \dot{E}x_{utilities,in} \tag{10}$$

As given by Equation (11), outlet exergy is associated with mass flow of products and residues.

$$\dot{E}x_{out} = \dot{E}x_{product,out} + \dot{E}x_{residues,out} \tag{11}$$

The total process irreversibilities measures the unused potential work as follows

$$\dot{E}x_{destroyed} = \dot{E}x_{in} - \dot{E}x_{product,out} \tag{12}$$

Non-evitable irreversibilities indicate the unused potential work without considering the exergy of residues

$$\dot{E}x_{loss} = \dot{E}x_{in} - \dot{E}x_{out} \tag{13}$$

The exergy efficiency of the process and the contribution of each stage to exergy loss were defined by Equations (14) and (15), respectively.

$$\eta_{exergy} = 1 - \left(\frac{Ex_{destroyed}}{Ex_{total,in}}\right) \tag{14}$$

$$\%Ex_{destroyed,i} = \left(\frac{Ex_{destroyed,i}}{Ex_{total,in}}\right) \times 100\% \tag{15}$$

2.3. Inherent Safety Assessment

The quantitative method selected to perform inherent safety assessment of the proposed biorefinery is the Numerical Descriptive Inherent Safety Technique (*NuDIST*), which was introduced by Ahmad et al. [33]. This approach considers both the chemical and process safety aspects that are quantified using Equations (16) and (17), respectively. The total *NuDIST* score corresponds to the sum of both *CSTS* and *PSTS*

$$CSTS = S_{FL} + S_{EP} + S_{TOX} \tag{16}$$

$$PSTS = S_T + S_P + S_{HR} \tag{17}$$

$$NuDIST\ score = CSTS + PSTS \tag{18}$$

where *CSTS* is the chemical safety total score, *PSTS* is the process safety total score, *S* is the score for flammability (*FL*), Explosiveness (*EP*), Toxicity (*TOX*), temperature (*T*), Pressure (*P*), and heat of reaction (*HR*). The logistic functions used to calculate these scores are given in Table 6. The input (x) refers to either the flash point, Upper Explosive Limit (UEL), Lower Explosive Limit (LEL), temperature, pressure, or heat of reaction.

Table 6. Logistic functions for *NuDIST* parameters.

Parameter	*Logistic Function*	*Input (x)*	
Flammability (S_{FL})	$S_{FL} = 100 \cdot \left(1 - \frac{1}{1+3.77e^{-0.024x}}\right)$	Flash point	(19)
Explosiveness (S_{EXP})	$S_{EXP} = 100 \cdot \left(1 - \frac{1}{1+1096.63e^{-0.14x}}\right)$	UEL-LEL	(20)
Toxicity (S_{TOX})	$S_{TOX} = 100 \cdot \left(1 - \frac{1}{1+403.4288e^{-0.012x}}\right)$	TLV-STEL	(21)
Temperature (S_T)	$S_{T>25°C} = 100 \cdot \left(\frac{1}{1+403.43e^{-0.012x}}\right)$	T (°C)	(22)
	$S_{T<25°C} = 100 \cdot \left(1 - \frac{1}{1+0.0025e^{-0.012x}}\right)$		(23)
Pressure (S_P)	$S_P = 100 \cdot \left(\frac{1}{1+148.41e^{-0.2x}}\right)$	P (bar)	(24)
Heat of Reaction (S_{HR})	$S_{HR>0\,\frac{kJ}{mol}} = 100 \cdot \left(\frac{1}{1+601.85e^{-0.016x}}\right)$	HR (kJ/mol)	(25)
	$S_{HR<0\,\frac{kJ}{mol}} = 100 \cdot \left(\frac{1}{1+403.43e^{-0.006x}}\right)$		(26)

3. Results and Discussion

3.1. Exergy Analysis

Figure 5 shows the contributions of each section to the irreversibilities, exergy input, exergy losses, exergy of wastes and utilities. This enabled the identification of critical processing steps within the shrimp-based biorefinery. The highest contribution (99.97%) to destroyed exergy was observed for the section (a) corresponding to the meat production units. Both beheading (S.3) and sorting (S.2) stages are responsible for this result due to the chemical exergy of high-molecular-weight components of stained/broken shrimps and heads. The stages belonging to the fresh shrimp processing operate at 9 °C (far from the reference state) to preserve the meat quality, leading to higher physical exergy. The above also applies for the parameters of exergy input and exergy of wastes, where Section (a) contributed the most, with 99.9%. Valorization alternatives for these residues encompass the production of shrimp oil rich in ω-3 fatty acids [34] and shrimp flour, which may serve to reduce the biowaste generation, and consequently, the exergy of wastes.

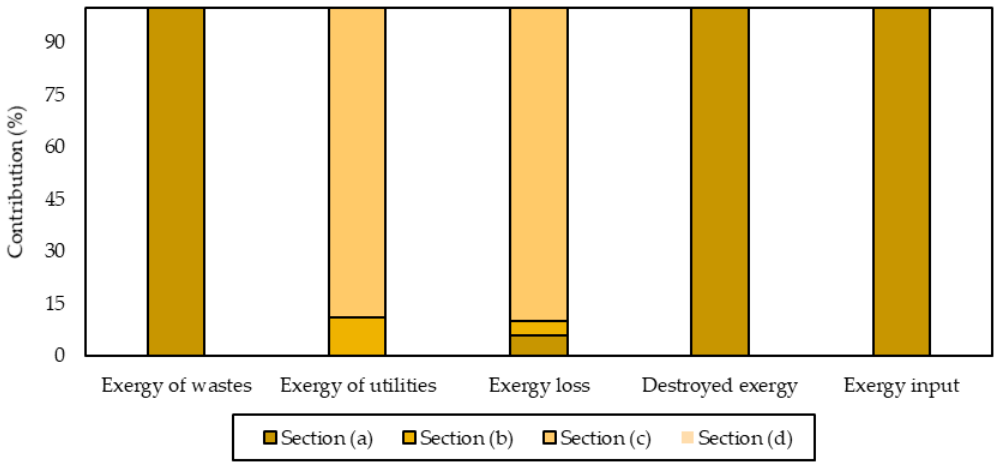

Figure 5. Contribution of process sections to the exergetic parameters.

Section (c) represents 89.8% and 88.8% of exergy loss and exergy of utilities, respectively, while accounting for the 0.03% of total irreversibilities. This is explained by the high energetic demand

for converting chitin into chitosan at a temperature of around 100–110 °C. The incorporation of heat integration approaches is key to reducing such irreversibilities by taking advantage of streams with high energetic potential. Section (b) shows a contribution of 11.25% and 4.27% for the exergy of utilities and exergy loss owed. The presence of multiple drying stages within shell processing increases the energetic consumption of this section, which supports the higher utility services entering the system compared with Section (d).

As is shown in Figure 6, the lowest exergy efficiencies were found for the deacetylation (S.10) and astaxanthin purification (S.13) stages, followed by beheading stage (S.3) with an efficiency around 26%. These stages showed small amount of exergy of products and high input exergy accounting for mass flow and utilities. The stages reaching the highest exergetic efficiencies are shrimp washing, peeling and depigmentation 1 and 2. Section (b) reported two stages with exergy efficiencies at 100%, while three stages reached values around 47–63%. Section (a) had no stages with null efficiencies, while Sections (c) and (d) show 0% efficiencies in one of the two constituent stages. Comparing these findings with the efficiency per stages for other systems, more stages have low exergetic performance in the shrimp-based biorefinery approach. For example, Moreno et al. (2019) [32] performed exergy analysis of two bio-oil systems reaching exergy efficiencies above 70% for most of the stages. Leal et al. (2019) [35] assessed an amine treatment unit showing exergy efficiencies above 90% excepting by the top circuit with 4.1%. Jia et al. (2017) [36] reported exergy efficiencies around 57.57–99.81% for units in the biodiesel production from barley straw.

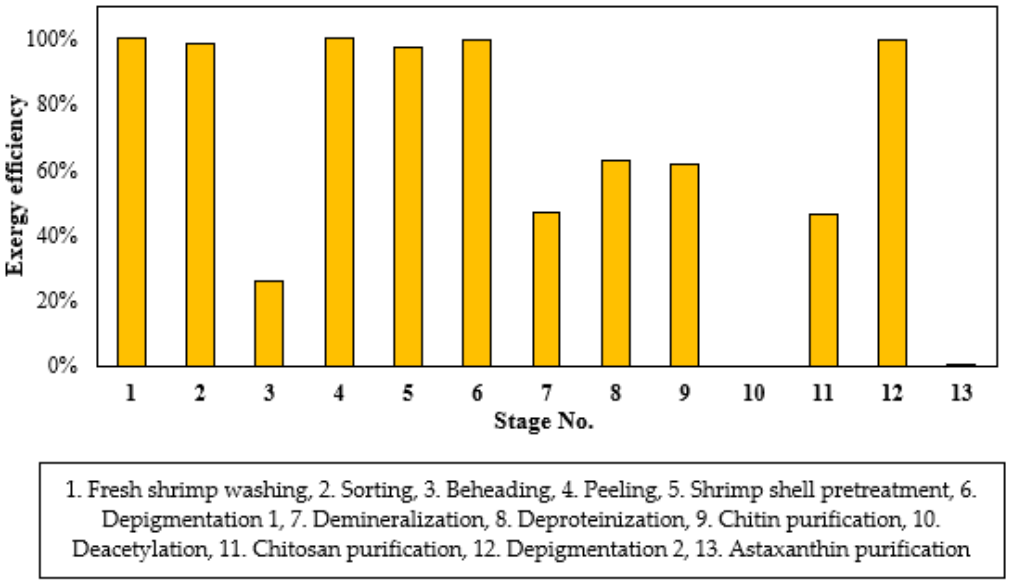

Figure 6. Exergy efficiency for shrimp-based biorefinery per stages.

Figure 7 depicts the process irreversibilities share per stage in the biorefinery approach. The beheading stage accounts for 98.325% of total irreversibilities, followed by the sorting stage, with 1.653%, which confirms the findings in the exergy analysis per section. Deacetylation stage reported a contribution of 0.029%, while fresh shrimp washing reached 0.002%. To reduce these irreversibilities, shrimp head usage is strongly recommended for further processing in the biorefinery as source of by-products or increasing the total amount of already considered products. The stages with minimal contribution are peeling (2.23×10^{-10}%), shell pretreatment (7.69×10^{-11}%), depigmentation 1 (5.38×10^{-12}%), and depigmentation 2 (9.43×10^{-12}%), and chitosan purification (3.12×10^{-4}%). The fact that shells from shrimp are employed for chitin, chitosan and astaxanthin production explains the lower irreversibilities of the peeling stage compared with beheading or sorting, where the same biomaterial is handled.

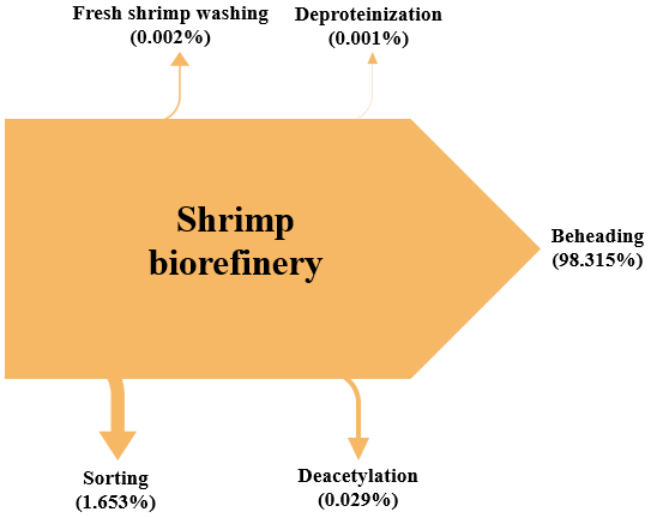

Figure 7. Sankey diagram of irreversibilities for shrimp biorefinery.

Figure 8 depicts a comparison between the overall exergy efficiency for shrimp biorefinery and other processes available in the literature [1,18,19,37]. The linear production of 12,152 t/y chitosan from shrimp shells reported by Meramo et al. (2020) [1] reached an efficiency at 4.6%, significantly lower than the efficiency obtained for the shrimp biorefinery at 24.6%. Despite this biorefinery approach showing a better global exergetic efficiency compared to the former process, its performance is worse than for palm oil-based biorefinery [18], lignocellulosic biorefineries [19] and microalgae oil extraction [37], with those reaching 59, 44 and 51%, respectively.

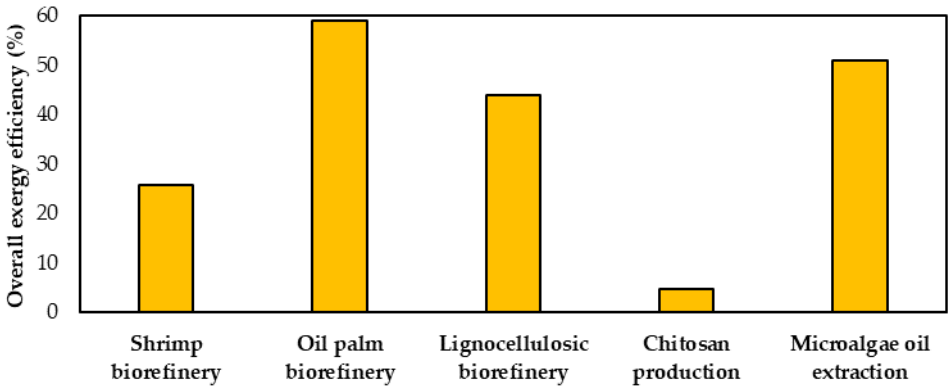

Figure 8. Comparison of overall exergy efficiencies.

3.2. Process Safety Assessment

Figure 9 shows flammability, explosiveness and toxicity scores for the substances handled per biorefinery section. The section reporting the highest score for flammability corresponds to astaxanthin recovery due to the use of acetone and ethanol. Section (b) also employs ethanol in the first depigmentation of shell; however, it reaches a lower flammability score (73.87). The explosiveness score for most sections is 0.81, which corresponds to the individual score for ethanol. Regarding the toxicity, Sections (a–c) reached a score of 99.75, followed by Section (d) with 99.39. The major contributors to these values are sodium hydroxide, calcium phosphate, phosphoric acid, and calcium chloride. The global safety performance of the biorefinery accounts for 85.31, 0.81 and 99.75 of S_{FL}, S_{EXP}, and S_{TOX}, respectively.

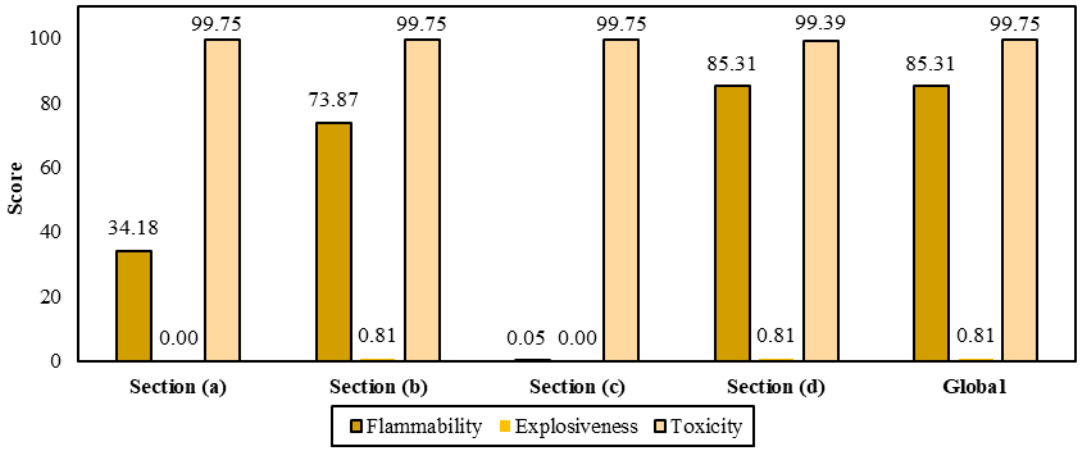

Figure 9. Scores for parameters associated with chemical safety.

The process safety analysis within the quantitative approach is depicted in Figure 10. Most biorefinery stages operate at environmental conditions; however, deacetylation reached a maximum temperature around 100–110 °C in the conversion reactor. The entire biorefinery operates at atmospheric pressure and, consequently, no hazard related to the working pressure in the system is associated to S_P score. It was found that the most exothermic main reaction in the biorefinery corresponds to the deacetylation reaction (HR = −4617 J/g), where chitin is transformed into chitosan by removing the acetyl groups present in it [30]. Section (b) corresponding to shell processing and chitin extraction reported the highest value for heat of reaction (108.10), followed by Section (c) with 100, where chitosan is obtained. The global scoring for temperature, pressure and heat of reaction was 0.8163, 0.8163 and 208.10, respectively.

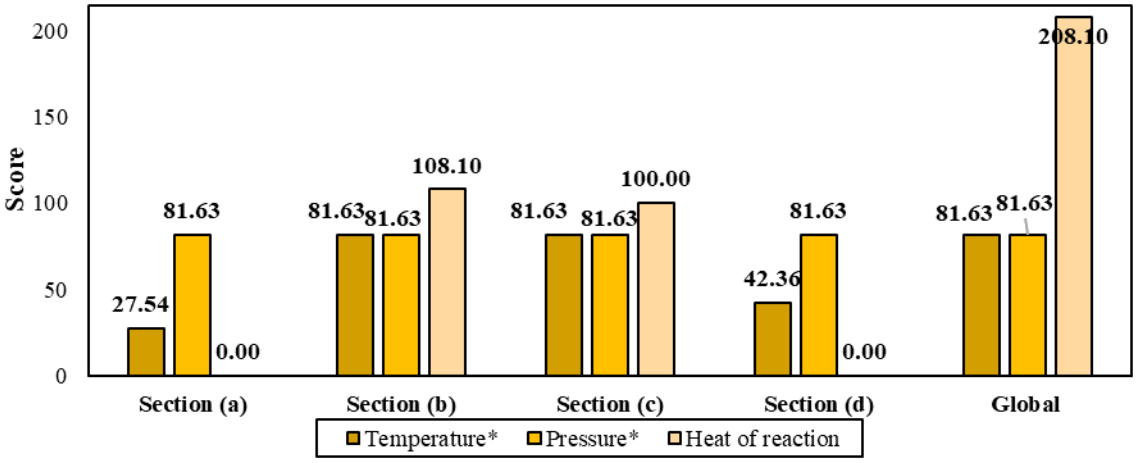

Figure 10. Scores for parameters associated with process safety (T and P × 10^{-2}).

The overall safety performance of the biorefinery approach is depicted in Figure 11. Section (b) reached the highest *NuDIST* score, with 445.79, followed by Section (c), with 363.05. This result is explained by the handling of more hazardous substances in the shell processing than for chitosan production. Section (d) reported the highest value for *CSTS* score, since the astaxanthin isolation is performed with acetone as extraction agent for ethanol and a pigment-rich mixture. These results were compared with the linear chitosan production from shrimp shells reported by Cassiani et al. (2020) [38]. They obtained a global *NuDIST* score of 380.20, lower than that obtained for the shrimp biorefinery (557.23), which is explained by the higher score given by acetone in stages of Section

(c). In general, the shrimp-based biorefinery showed a moderate level of risk that is similar to the performance analyzed for routes of propylene (C3) by Ahmad et al. (2014) [39].

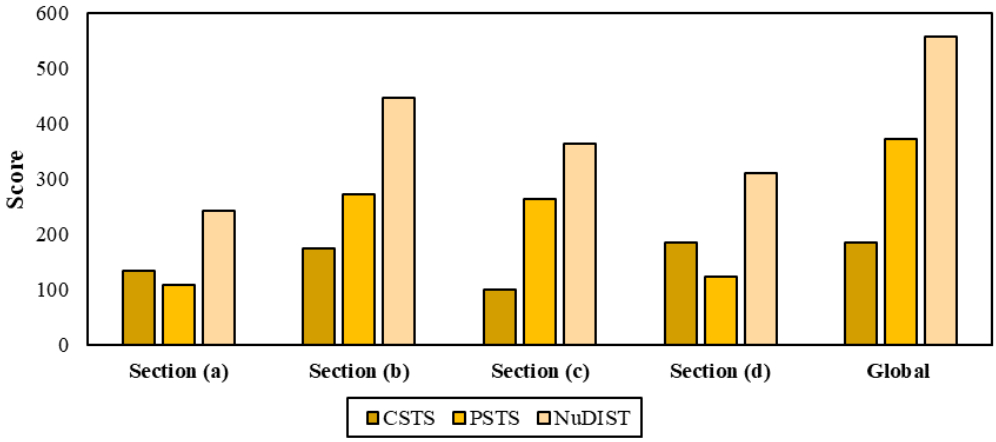

Figure 11. Estimation of *NuDIST* score per process section.

4. Conclusions

This work was focused on the development of a safety assessment of a pilot-scale shrimp-based biorefinery that produces shrimp meat and value-added products using the inherent safety index method to evaluate the social component of sustainability for this process. The biorefinery was designed to process 4534 t/year of fresh shrimp and was simulated in Aspen Plus® software. The approach showed a moderate level of risk (557.23), mainly associated with the handling of ethanol and acetone. The evaluation of a different solvent than acetone in the second depigmentation could improve the intrinsic safety of the process. The overall exergy efficiency was quantified at 25.61%, which is higher than chitosan-from-exoskeleton linear production chain (4.58%). The highest exergy losses were found on stages as deacetylation, fresh shrimp washing and deproteinization stages. The beheading stage most contributed to the irreversibilities, with 98.315%, followed by sorting, with 1.653%.

Author Contributions: Conceptualization, Á.D.G.-D. and J.D.M.-C.; methodology, Á.D.G.-D.; software, K.A.M.-S.; validation, Á.D.G.-D., K.A.M.-S. and J.D.M.-C.; formal analysis, K.A.M.-S.; investigation, K.A.M.-S.; resources, Á.D.G.-D.; data curation, Á.D.G.-D.; writing—original draft preparation, K.A.M.-S.; writing—review and editing, Á.D.G.-D.; visualization, J.D.M.-C.; supervision, Á.D.G.-D.; project administration, Á.D.G.-D.; funding acquisition, J.D.M.-C. All authors have read and agreed to the published version of the manuscript.

Funding: This research was funded by Corporación Universitaria Minuto De Dios Uniminuto, grant number C119-154 and The APC was funded by UNIMINUTO.

Acknowledgments: The authors thank to University of Cartagena and Corporación Universitaria Minuto de Dios UNIMINUTO for providing equipment and software for successfully conclude this research.

Conflicts of Interest: The authors declare no conflict of interest.

References

1. Meramo-Hurtado, S.; Alarcón-Suesca, C.; González-Delgado, Á.D. Exergetic sensibility analysis and environmental evaluation of chitosan production from shrimp exoskeleton in Colombia. *J. Clean. Prod.* **2020**, *248*, 119285. [CrossRef]
2. Kandra, P.; Challa, M.M.; Kalangi Padma Jyothi, H. Efficient use of shrimp waste: Present and future trends. *Appl. Microbiol. Biotechnol.* **2012**, *93*, 17–29. [CrossRef] [PubMed]
3. Mao, X.; Guo, N.; Sun, J.; Xue, C. Comprehensive utilization of shrimp waste based on biotechnological methods: A review. *J. Clean. Prod.* **2017**, *143*, 814–823. [CrossRef]

4. Molino, A.; Mehariya, S.; Iovine, A.; Larocca, V.; Di Sanzo, G.; Martino, M.; Casella, P.; Chianese, S.; Musmarra, D. Extraction of Astaxanthin and Lutein from Microalga Haematococcus pluvialis in the Red Phase Using CO_2 Supercritical Fluid Extraction Technology with Ethanol as Co-Solvent. *Mar. Drugs* **2018**, *16*, 432. [CrossRef] [PubMed]
5. Maschmeyer, T.; Luque, R.; Selva, M. Upgrading of marine (fish and crustaceans) biowaste for high added-value molecules and bio(nano)-materials. *Chem. Soc. Rev.* **2020**, *49*, 4527–4563. [CrossRef]
6. Machmudah, S.; Wahyudiono; Kanda, H.; Goto, M. Supercritical fluids extraction of valuable compounds from algae: Future perspectives and challenges. *Eng. J.* **2018**, *22*, 13–30. [CrossRef]
7. Wu, L.; Li, L.; Chen, S.; Wang, L.; Lin, X. Deep eutectic solvent-based ultrasonic-assisted extraction of phenolic compounds from Moringa oleifera L. leaves: Optimization, comparison and antioxidant activity. *Sep. Purif. Technol.* **2020**, *247*, 117014. [CrossRef]
8. Molino, A.; Mehariya, S.; Di Sanzo, G.; Larocca, V.; Martino, M.; Leone, G.P.; Marino, T.; Chianese, S.; Balducchi, R.; Musmarra, D. Recent developments in supercritical fluid extraction of bioactive compounds from microalgae: Role of key parameters, technological achievements and challenges. *J. CO2 Util.* **2020**, *36*, 196–209. [CrossRef]
9. IEA Bioenergy. Sustainable and synergetic processing of biomass into marketable food & feed ingredients, products (chemicals, materials) and energy (fuels, power, heat). In *Task42 Biorefining*; International Energy Agency: Wageningen, The Netherlands, 2014.
10. Ubando, A.T.; Felix, C.B.; Chen, W.-H. Biorefineries in circular bioeconomy: A comprehensive review. *Bioresour. Technol.* **2020**, *299*, 122585. [CrossRef]
11. Paone, E.; Tabanelli, T.; Mauriello, F. The rise of lignin biorefinery. *Curr. Opin. Green Sustain. Chem.* **2020**, *24*, 1–6. [CrossRef]
12. Rathnayaka, S.; Khan, F.; Amyotte, P. Risk-based process plant design considering inherent safety. *Saf. Sci.* **2014**, *70*, 438–464. [CrossRef]
13. Niño-Villalobos, A.; Puello-Yarce, J.; González-Delgado, A.; Ojeda, K.; Sánchez-Tuirán, E. Biodiesel and Hydrogen Production in a Combined Palm and Jatropha Biomass Biorefinery: Simulation, Techno-Economic, and Environmental Evaluation. *ACS Omega* **2020**, *5*, 7074–7084. [CrossRef] [PubMed]
14. Meramo-Hurtado, S.; Herrera-Barros, A.; González-Delgado, Á. Evaluation of large-scale production of chitosan microbeads modified with nanoparticles based on exergy analysis. *Energies* **2019**, *12*, 1200. [CrossRef]
15. Bi, Y.; Chen, L.; Sun, F. Exergetic efficiency optimization for an irreversible heat pump working on reversed Brayton cycle. *Pramana* **2010**, *74*, 351–363. [CrossRef]
16. Dincer, I.; Abu-Rayash, A. Chapter 6—Sustainability modeling. In *Energy Sustainability*; Dincer, I., Abu-Rayash, A.B.T.-E.S., Eds.; Academic Press: Cambridge, MA, USA, 2020; pp. 119–164, ISBN 978-0-12-819556-7.
17. Li, X.; Zanwar, A.; Jayswal, A.; Lou, H.H.; Huang, Y. Incorporating exergy analysis and inherent safety analysis for sustainability assessment of biofuels. *Ind. Eng. Chem. Res.* **2011**, *50*, 2981–2993. [CrossRef]
18. Ofori-Boateng, C.; Lee, K.T. An oil palm-based biorefinery concept for cellulosic ethanol and phytochemicals production: Sustainability evaluation using exergetic life cycle assessment. *Appl. Therm. Eng.* **2014**, *62*, 90–104. [CrossRef]
19. Aghbashlo, M.; Mandegari, M.; Tabatabaei, M.; Farzad, S.; Mojarab, M.; Johann, F.G. Exergy analysis of a lignocellulosic-based biore fi nery annexed to a sugarcane mill for simultaneous lactic acid and electricity production. *Energy* **2018**, *149*, 623–638. [CrossRef]
20. Salvatore, D.; Bubbico, R.; Di, L. Environmental and Safety Aspects of Integrated BioRefineries (IBR) in Italy. *Chem. Eng. Trans.* **2013**, *32*, 169–174.
21. Lauri, R.; Pietrangeli, B. Biorefinery Safety: A Case Study Focused on Bioethanol Production. In *Biorefinery Concepts, Energy and Products*; IntechOpen: London, UK, 2019.
22. Meramo-Hurtado, S.I.; Sanchez-Tuiran, E.; Ponce-Ortega, J.M.; El-Halwagi, M.M.; Ojeda-Delgado, K.A. Synthesis and Sustainability Evaluation of a Lignocellulosic Multifeedstock Biorefinery Considering Technical Performance Indicators. *ACS Omega* **2020**, *5*, 9259–9275. [CrossRef]
23. Pinedo, J.; García Prieto, C.V.; D'Alessandro, A.A.; Ibáñez, R.; Tonelli, S.; Díaz, M.S.; Irabien, Á. Microalgae biorefinery alternatives and hazard evaluation. *Chem. Eng. Res. Des.* **2016**, *107*, 117–125. [CrossRef]
24. González, B. Producción Local de Camarón Completó Cuatro Años al Alza, Aumentó de 21% Comparado con 2017. Available online: https://www.agronegocios.co/agricultura/ (accessed on 10 October 2020).

25. Bonfante-Alvarez, H.; De Avila-Montiel, G.; Herrera-Barros, A.; Torrenegra-Alarcón, M.; González-Delgado, Á.D. Evaluation of five chitosan production routes with astaxanthin recovery from shrimp exoskeletons. *Chem. Eng. Trans.* **2018**, *70*, 1969–1974.
26. Naciones Unidas Organización de Desarrollo Industrial (ONUDI). Guía de Recursos Eficientes y Producción más Limpia. Sector Camaronero. 2017, pp. 1–74. Available online: https://open.unido.org/api/documents/13020765/download/Gu%C3%ADa%20para%20la%20eficiencia%20de%20recursos%20y%20producci%C3%B3n%20m%C3%A1s%20limpia%20en%20el%20sector%20camaronero.pdf (accessed on 10 October 2020).
27. Díaz Rengifo, P.M. *Utilización del Metabisulfito de Sodio Como Preservante en las Camaroneras*; Universidad Agraria del Ecuador: Guayaquil, Ecuador, 2009.
28. Lim Law, C.; Mujumdar, A.S. Fluidized Bed Dryers. In *Handbook of Industrial Drying*; Mujumdar, A.S., Ed.; Taylor & Frnacis Group: New York, NY, USA, 2006; pp. 173–201.
29. Srinivasan, H.; Kanayairam, V.; Ravichandran, R. Chitin and chitosan preparation from shrimp shells Penaeus monodon and its human ovarian cancer cell line, PA-1. *Int. J. Biol. Macromol.* **2018**, *107*, 662–667. [CrossRef] [PubMed]
30. Hossain, M.S.; Iqbal, A. Production and characterization of chitosan from shrimp waste. *J. Bangladesh Agric. Univ.* **2014**, *12*, 153–160. [CrossRef]
31. Aghbashlo, M.; Mobli, H.; Rafiee, S.; Madadlou, A. A review on exergy analysis of drying processes and systems. *Renew. Sustain. Energy Rev.* **2013**, *22*, 1–22. [CrossRef]
32. Moreno-Sader, K.; Meramo-Hurtado, S.I.; González-Delgado, A.D. Computer-aided environmental and exergy analysis as decision-making tools for selecting bio-oil feedstocks. *Renew. Sustain. Energy Rev.* **2019**, *112*, 42–57. [CrossRef]
33. Ahmad, S.I.; Hashim, H.; Hassim, M.H.; Abdul, Z. Inherent Safety Assessment of Biodiesel Production: Flammability Parameter. *Procedia Eng.* **2016**, *148*, 1177–1183. [CrossRef]
34. Scurria, A.; Tixier, A.F.; Lino, C.; Pagliaro, M.; Agostino, F.D.; Avellone, G.; Ciriminna, R. High Yields of Shrimp Oil Rich in Omega-3 and Carotenoids: Extending to Shrimp Waste the Circular Economy Approach to Fish Oil Extraction. *ACS Omega* **2020**, 1–7. [CrossRef]
35. Leal-Navarro, J.; Mestre-Escudero, R.; Puerta-Arana, A.; León-Pulido, J.; González-Delgado, Á.D. Evaluating the Exergetic Performance of the Amine Treatment Unit in a Latin-American Refinery. *ACS Omega* **2019**, *4*, 21993–21997. [CrossRef]
36. Jia, Z.; Chi, R.; Sun, L.; Tan, H. Biodiesel processes energy improvement based on Pinch and exergy Analysis. *Chem. Eng. Trans.* **2017**, *61*, 487–492.
37. Peralta-Ruiz, Y.; Gonzalez-Delgadi, A.; Kafarov, V. Evaluation of alternatives for microalgae oil extraction based on exergy analysis. *Appl. Energy* **2013**, *101*, 226–236. [CrossRef]
38. Zuorro, A.; Cassiani-cassiani, D.; Meza-gonz, D.A. Evaluation of Shrimp Waste Valorization Combining Computer-Aided Simulation and Numerical Descriptive Inherent Safety Technique (NuDIST). *Appl. Sci.* **2020**, *10*, 5339. [CrossRef]
39. Ahmad, S.I.; Hashim, H.; Hassim, M.H. Numerical Descriptive Inherent Safety Technique (NuDIST) for inherent safety assessment in petrochemical industry. *Process Saf. Environ. Prot.* **2014**, *92*, 379–389. [CrossRef]